Spectroscopic Studies of Copper(II) Bound at the Native Copper Site or Substituted at the Native Zinc Site of Bovine Erythrocuprein (Superoxide Dismutase)

Michael W. Pantoliano,[1] Joan S. Valentine,*[2] and Laurence A. Nafie[3]

Contribution from the Departments of Chemistry, Rutgers University, New Brunswick, New Jersey 08903, and Syracuse University, Syracuse, New York 13210, and the Department of Chemistry and Biochemistry and Molecular Biology Institute, University of California, Los Angeles, California 90024. *Received January 29, 1982*

Abstract: Electronic and ESR spectroscopy have been used to characterize the ligand environments of Cu^{II} bound at the native Cu or Zn sites of bovine erythrocuprein (superoxide dismutase). The near-UV and visible absorption and circular dichroism spectra of the native $Cu^{II}_2Zn^{II}_2$ and zinc-free proteins are reexamined in light of a recent study of the electronic absorption spectra of tetragonal Cu^{II}–imidazole and Cu^{II}–imidazolate model compounds (Fawcett, T. G.; Bernarducci, E. E.; Krogh-Jespersen, K.; Schugar, H. J. *J. Am. Chem. Soc.* **1980**, *102*, 2598–2604). Assignments are made in the spectrum of the native $Cu^{II}_2Zn^{II}_2$ protein for the weak but broad shoulders at 340 and 420 nm to imidazole (π) to Cu^{II} and imidazolate to Cu^{II} ligand-to-metal charge transfer (LMCT) transitions, respectively. Copper(II) bound at the Zn site in the $Ag^{I}_2Cu^{II}_2$ and four-Cu derivatives is found to give a broad and moderately intense band ($\epsilon \sim 2000\ M^{-1}\ cm^{-1}$) at approximately 300 nm, believed to arise from carboxylate (COO^-) to Cu^{II} and/or imidazole (π) to Cu^{II} LMCT transitions. Ligand-field transitions at 835, 1000, and 1250 nm in the near-IR spectrum, together with a distinctly rhombic ESR signal and small hyperfine coupling constant ($10.2 \times 10^{-3}\ cm^{-1}$ at 30 °C), suggest that Cu^{II} bound to the Zn site in the $Ag^{I}_2Cu^{II}_2$ protein is in an environment significantly distorted from tetragonal toward a tetrahedral or distorted-pentacoordinate geometry. Some resemblances of the spectral properties of Cu^{II} in the $Ag^{I}_2Cu^{II}_2$ protein with those of modified type 3 copper centers are also noted.

Cupric ion has proven to be a particularly useful spectroscopic probe of the metal ion binding sites of copper proteins and of copper-substituted zinc or iron metalloproteins. Analysis of the ESR,[4] absorption, and circular dichroism (CD) spectra[5-9] has provided invaluable information concerning the electronic and geometric nature of the metal ion binding sites of these copper-containing proteins. Our continuing interest in bovine erythrocuprein, $Cu^{II}_2Zn^{II}_2$BE,[10] and its metal-substituted derivatives[11-13] has led us to undertake a more detailed examination of the electronic spectra of several of these species. Although other investigators[14-24] have reported some of the spectra that we report here, firm assignments of the electronic transitions of copper bound at the native Cu site were not previously possible. A recent detailed study of the near-UV spectra of Cu^{II}–imidazole and Cu^{II}–imidazolate complexes in solution and in the solid state by Schugar and co-workers[25,26] has provided the necessary background for assignment of the optical transitions observed in the electronic absorption and CD spectra of $Cu^{II}_2Zn^{II}_2$BE, $Cu^{II}_2E_2$BE, $Cu^{II}_2Cu^{II}_2$BE, and $Ag^{I}_2Cu^{II}_2$BE.[27]

The $Cu^{II}_2Cu^{II}_2$BE and $Ag^{I}_2Cu^{II}_2$BE derivatives have proven to be particularly interesting for spectral studies because they contain Cu^{II} bound at the native Zn site. We have found that the spectroscopic properties of Cu^{II} bound to the native Zn site of bovine erythrocuprein are unusual compared to most copper-containing proteins and, in addition, that they show an interesting resemblance to the spectroscopic properties of partially reduced type 3 binuclear copper centers of fungal and tree laccases and cytochrome *c* oxidase. These results are also the subject of this paper.

Experimental Section

Bovine erythrocuprein was purified and characterized as described previously.[13] Metal-substituted derivatives were prepared as before[13]

(1) Present address: Center for Biochemical and Biophysical Sciences and Medicine, Harvard Medical School, Boston, MA 02115.
(2) Present address: Department of Chemistry, University of California, Los Angeles, CA 90024.
(3) Syracuse University.
(4) (a) Vänngård, T. In "Biological Applications of Electron Spin Resonance"; Swartz, H. M., Bolton, J. R., Borg, D. C., Eds.; Wiley-Interscience: New York, 1972; pp 411–447. (b) Boas, J. F.; Pilbrow, J. R.; Smith, T. D. In "Biological Magnetic Resonance"; Berliner, L. J., Reuben, J., Eds.; Plenum Press: New York, 1978; pp 277–342.
(5) Rosenberg, R. C.; Root, C. A.; Bernstein, P. K.; Gray, H. B. *J. Am. Chem. Soc.* **1975**, *97*, 2092–2096.
(6) Solomon, E. I.; Hare, J. W.; Gray, H. B. *Proc. Natl. Acad. Sci. U.S.A.* **1976**, *73*, 1389–1393.
(7) Solomon, E. I.; Hare, J. W.; Dooley, D. M.; Dawson, J. H.; Stephens, P. J.; Gray, H. B. *J. Am. Chem. Soc.* **1980**, *102*, 168–178.
(8) Dooley, D. M.; Rawlings, J.; Dawson, J. H.; Stephens, P. J.; Andréasson, L. E.; Malmström, B. G.; Gray, H. B. *J. Am. Chem. Soc.* **1979**, *101*, 5038–5046.
(9) Dawson, J. H.; Dooley, D. M.; Clark, R.; Stephens, P. J.; Gray, H. B. *J. Am. Chem. Soc.* **1979**, *101*, 5046–5053.
(10) Abbreviations used in this paper are as follows: $Cu^{II}_2Zn^{II}_2$BE designates bovine erythrocuprein as isolated from erythrocytes. In general, X_2Y_2BE designates derivatives of erythrocuprein in which the metal ions X and Y have been substituted for Cu^{II} and Zn^{II}, respectively (X and Y may be the same); Cu_2E_2BE designates the zinc-free derivative of bovine erythrocuprein in which the Zn site is vacant (E = empty); ImH, imidazole; Im^-, imidazolate.
(11) Valentine, J. S.; Pantoliano, M. W.; McDonnell, P. J.; Burger, A. R.; Lippard, S. J. *Proc. Natl. Acad. Sci. U.S.A.* **1979**, *76*, 4245–4249.
(12) Pantoliano, M. W.; McDonnell, P. J.; Valentine, J. S. *J. Am. Chem. Soc.* **1979**, *101*, 6454–6456.
(13) Pantoliano, M. W.; Valentine, J. S.; Mammone, R. J.; Scholler, D. M. *J. Am. Chem. Soc.* **1982**, *104*, 1717–1723.
(14) McCord, J. M.; Fridovich, I. *J. Biol. Chem.* **1969**, *244*, 6049–6055.
(15) Bannister, J.; Bannister, W.; Wood, E. *Eur. J. Biochem.* **1971**, *18*, 178–186.
(16) Wood, E.; Dalgleish, D.; Bannister, W. *Eur. J. Biochem.* **1971**, *18*, 187–193.
(17) Weser, U.; Schubotz, L. M. *Bioinorg. Chem.* **1978**, *9*, 505–519.
(18) (a) Fee, J. A. *J. Biol. Chem.* **1973**, *248*, 4229–4234. (b) Fee, J. A. *Biochim. Biophys. Acta* **1973**, *295*, 87–95.
(19) (a) Fee, J. A. In "Superoxide and Superoxide Dismutases"; Michelson, A. M., McCord, J. M., Fridovich, I., Eds.; Academic Press: New York, 1977, pp 173–192. (b) Fee, J. A. *Met. Ions Biol. Sys.* **1981**, *13*, 259–298.
(20) Weser, U.; Bunnenberg, E.; Cammack, R.; Djerassi, C.; Flohé, L.; Thomas, G.; Voelter, W. *Biochim. Biophys. Acta* **1971**, *243*, 203–213.
(21) Rotilio, G.; Finazzi-Agrō, A.; Calabrese, L.; Bossa, F.; Guerrieri, P.; Mondovi, B. *Biochemistry* **1971**, *10*, 616–621.
(22) Rotilio, G.; Calabrese, L.; Coleman, J. E. *J. Biol. Chem.* **1973**, *248*, 3855–3859.
(23) Beem, K. M.; Rich, W. E.; Rajagopalan, K. V. *J. Biol. Chem.* **1974**, *249*, 7298–7305.
(24) Beem, K. M.; Richardson, D. C.; Rajagopalan, K. V. *Biochemistry* **1977**, *16*, 1930–1936.
(25) Fawcett, T. G.; Bernarducci, E. E.; Krogh-Jespersen, K.; Schugar, H. J. *J. Am. Chem. Soc.* **1980**, *102*, 2598–2604.
(26) Bernarducci, E.; Schwindinger, W. F.; Hughey, J. L; Krogh-Jespersen, K.; Schugar, H. J. *J. Am. Chem. Soc.* **1981**, *103*, 1686–1691.
(27) For a review of metal substitutions in $Cu^{II}_2Zn^{II}_2$BE, see: Valentine, J. S.; Pantoliano, M. W. In "Copper Proteins"; Spiro, T. G., Ed.; Wiley-Interscience: NY, 1981; pp 292–358.

0002-7863/82/1504-6310$01.25/0

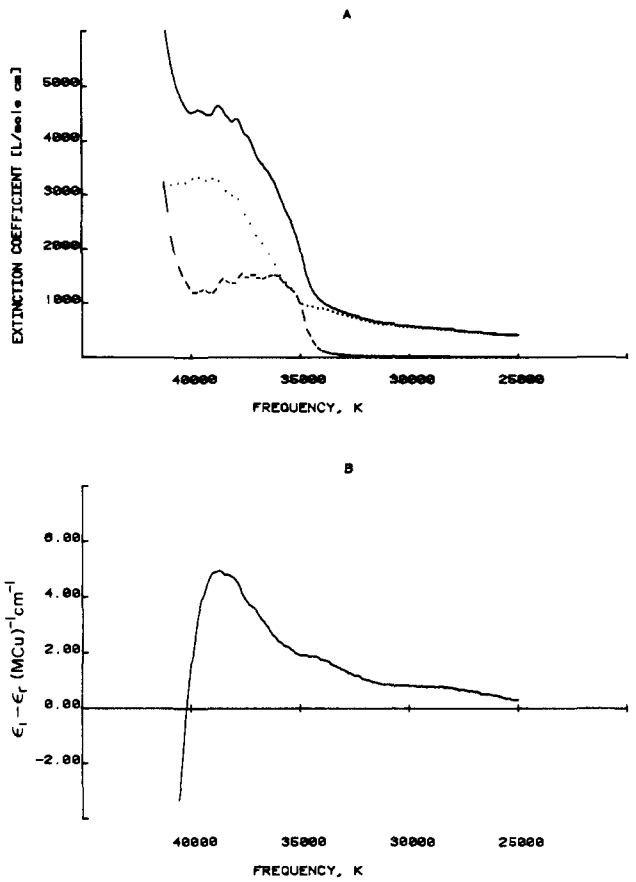

Figure 1. (A) Near-UV absorption spectrum of $Cu^{II}_2Zn^{II}_2BE$ (—) and apoprotein (---). A $Cu^{II}_2Zn^{II}_2BE$ minus apoprotein difference spectrum (···) was generated from these two spectra by digital subtraction. The $Cu^{II}_2Zn^{II}_2BE$ spectrum was obtained by using a 0.10-cm quartz cuvette filled with a 1.02 mM (subunits) solution buffered at pH 6.1 in 50 mM potassium phosphate. The apoprotein spectrum was obtained with a 1.0-cm quartz cuvette filled with a 0.27 mM (subunits) solution buffered at pH 3.7 in 10 mM sodium acetate. The extinction coefficients were calculated by using the concentration of protein subunits, and no correction was made for only 85% occupancy of Cu in the Cu binding site of $Cu^{II}_2Zn^{II}_2BE$. (B) Near-UV circular dichroism spectrum of $Cu^{II}_2Zn^{II}_2BE$. This spectrum was obtained for the same $Cu^{II}_2Zn^{II}_2BE$ solution described above.

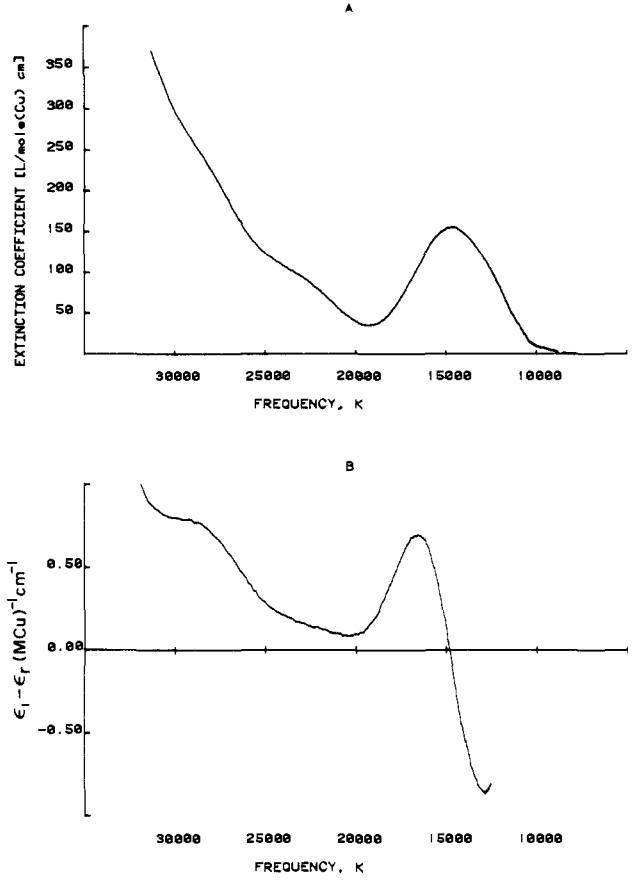

Figure 2. (A) Visible and near-IR absorption spectrum of $Cu^{II}_2Zn^{II}_2BE$ at pH 6.1. The same $Cu^{II}_2Zn^{II}_2BE$ solution described in Figure 1 was used to obtain this spectrum. A 1.0-cm quartz cuvette was used. (B) Visible and near-IR circular dichroism spectrum of $Cu^{II}_2Zn^{II}_2BE$ at pH 6.1. The same $Cu^{II}_2Zn^{II}_2BE$ solution was also used to obtain this spectrum. See Experimental Section for details.

except that the Zn-free derivative ($Cu^{II}_2E_2BE$) was prepared by dialysis of $Cu^{II}_2Zn^{II}_2BE$ at pH 3.6.[12] $Ag^{I}_2Cu^{II}_2BE$ was prepared by a modification of the procedure of Beem et al.,[24] which is described in detail under Results. All solutions were prepared with doubly-distilled deionized water, and the usual precautions were taken throughout to avoid contamination by adventitious metal ions.[13]

Absorption spectra were recorded with a Cary 17D spectrophotometer at ambient temperature. Protein solutions (except those in D_2O) were filtered through a 0.22-μm filter (MF, Millipore) before spectral observations. Extinction coefficients were calculated in each case on the basis of Cu found by atomic absorption (AA) photometry except in the case of $Cu^{II}_2Cu^{II}_2BE$ where the extinction coefficient is reported on the basis of the concentration of the protein subunits.

Visible and near-ultraviolet (UV) circular dichroism (CD) spectra were recorded at ambient temperature with a Cary 61 spectropolarimeter. Spectra were obtained in the visible region (300–800 nm) with a 1.0-cm quartz cell. The instrument sensitivity was set in this case for a maximum pen deflection of ±0.05° or 0.10° ellipticity. The slit width was programmed by the manufacturer to give a constant spectral bandwidth of about 2 nm. At 800 nm (12 500 cm^{-1}), the slit width was set at 0.35 mm; it increased according to the slit program to 1.0 mm at 670 nm (14 900 cm^{-1}). At 670 nm, the slit width was set at 0.1 mm, and it increased according to the slit program to 1.0 mm at 300 nm (33 300 cm^{-1}). CD spectra in the near UV were obtained with a 0.20-cm quartz cell. The instrument sensitivity in this case was set for a maximum pen deflection of ±0.025, and the slit width was set at 0.5 mm at 400 nm; it increased according to the slit program to 1.2 mm at 240 nm (41 700 cm^{-1}). The largest value of the dynode voltage was 0.4 kV at 240 nm.

Circular dichroism is expressed as $\epsilon_l - \epsilon_r$ with units M^{-1} cm^{-1} and calculated from the following equation:

$$\epsilon_l - \epsilon_r = \frac{[\theta]}{2.303(4500/\pi)}$$

$[\theta]$ is the molecular ellipticity and is defined as

$$[\theta] = \frac{\theta^\circ}{10}\frac{M_r}{lc'}$$

where θ° is the measured ellipticity in degrees, M_r is the molecular weight of the sample (15 700), c' is the concentration in g/cm^3, and l is the pathlength of the sample solution in cm. The CD spectra reported here are the average of two different scans and are calculated on the basis of the concentration of Cu found by AA analysis. Calibration of the instrument was performed with a 0.10% aqueous solution of reagent grade *d*-10-camphorsulfonic acid (Baker) that had previously been dried over P_2O_5 under reduced pressure.

Near-infrared CD measurements were obtained at ambient temperature with a laboratory-constructed instrument that is an adaptation of one previously described.[28,29] Calibration of the instrument was performed as described by Nafie et al.[29], and the sensitivity was set at $\Delta A = 1 \times 10^{-4}$ for the region 870–1800 nm. Liquid-nitrogen and ambient-temperature ESR spectra were obtained as described elsewhere.[13] A Corning Model 12 pH meter and a thin (6 mm) Sensorex combination glass electrode were employed for pH measurements. D_2O (99.8% D) was purchased from Bio-Rad (Biological Grade). Reagent grade chemicals were used throughout without further purification.

(28) Osborne, G. A.; Cheng, J. C.; Stephens, P. J. *Rev. Sci. Instrum.* **1973**, *44*, 10–15.
(29) Nafie, L. A.; Keiderling, T. A.; Stephens, P. J. *J. Am. Chem. Soc.* **1976**, *98*, 2715–2723.

Table I. Electronic Transition Assignments for Bovine Erythrocuprein and Derivatives

derivative	frequency, 10^{-3} cm^{-1}, (λ, nm)[a]	ϵ,[b] (M Cu)$^{-1}$ cm^{-1}	$\epsilon_l - \epsilon_r$, (M Cu)$^{-1}$ cm^{-1}	assignment
$Cu^{II}_2Zn^{II}_2BE$ (pH 6.1)	39.0 (256)	3300	+4.9	π(ImH) → Cu LMCT
	35.0 (286)	1000	+1.9	π(ImH) → Cu LMCT
	29.5 (339)	250	+0.79	π(ImH) → Cu LMCT
	24.0 (417)	110	+0.23	Im$^-$ → Cu LMCT
	18.8 (532)		+0.21	Cu d–d
	16.4 (610)	155[c]	+0.70	Cu d–d
	13.0 (770)		−0.86	Cu d–d
$Cu^{II}_2E_2BE$ (pH 3.6)	39.0 (256)		+6.9	π(ImH) → Cu LMCT
	32.0 (313)	225	+0.69	π(ImH) → Cu LMCT
	17.0 (588)		+0.15	Cu d–d
	13.5 (741)	131[c]	−0.47	Cu d–d
$Cu^{II}_2E_2BE$ (pH 6.7)	31.0 (323)	225	+0.54	π(ImH) → Cu LMCT
	18.0 (556)		+0.06	Cu d–d
	16.2 (617)	124[c]	+0.31	Cu d–d
	<12.5 (>800)		<−0.44	Cu d–d
$Ag^{I}_2Cu^{II}_2BE$ (pH 6.2)	>40.0 (<250)	>2000		
	33.8 (296)	1800	+1.94	π(ImH) and COO$^-$ → Cu LMCT
	26.5 (377)	250	+0.21	π(ImH) → Cu LMCT
	12.0 (830)	100[c]	−1.47	Cu d–d
	10.0 (1000)		+1.64	Cu d–d
	8.0 (1250)		+0.38	Cu d–d

[a] Band positions are from near-UV, visible, and near-IR CD spectra. [b] Extinction coefficients for bands in the visible region are based on the amount of Cu bound per subunit; thus the units are (M Cu)$^{-1}$ cm^{-1}. [c] For maximum of ligand field envelope.

Results and Discussion

Optical Properties of $Cu^{II}_2Zn^{II}_2BE$. The near-UV absorption spectrum of $Cu^{II}_2Zn^{II}_2BE$ and apoprotein are shown in Figure 1A. These spectra are very similar to those reported previously by McCord and Fridovich.[14] A digital substraction of the apoprotein spectrum from that of $Cu^{II}_2Zn^{II}_2BE$ is also shown in Figure 1A. This difference spectrum and the visible–UV spectrum of $Cu^{II}_2Zn^{II}_2BE$ shown in Figure 2A reveal a minimum of three very broad bands of varying intensities in the UV region. The most intense band appears at 39 000 cm^{-1} (256 nm) with $\Delta\epsilon$ = 3300 M^{-1} cm^{-1}. Less intense shoulders appear at 35 000 cm^{-1} (286 nm) with $\Delta\epsilon$ = 1000 M^{-1} cm^{-1} and at 29 500 cm^{-1} (339 nm) with $\Delta\epsilon$ = 300 M^{-1} cm^{-1}. The near-UV CD spectrum of $Cu^{II}_2Zn^{II}_2BE$ is shown in Figure 1B. It bears a strong resemblance to the absorption difference spectrum in Figure 1A with the expected increased resolution characteristic of the more narrow CD bandwidths.[30]

The visible-absorption and CD bands of $Cu^{II}_2Zn^{II}_2BE$ are shown in Figure 2, A and B, respectively. In addition to the shoulder at 29 500 cm^{-1} already mentioned, another less intense shoulder appears at 24 000 cm^{-1} (417 nm) as well as a broad maximum at 14 700 cm^{-1} (680 nm). The CD spectrum gives better resolution of the bands found in the absorption spectrum, as expected. The broad positive band centered at 29 500 cm^{-1} is more easily seen in the CD spectrum than in the absorption spectrum. Less resolved, but nevertheless apparent, in the CD spectrum is a shoulder at 24 000 cm^{-1}. The broad maximum centered at 14 700 cm^{-1} in the absorption spectrum is resolved into at least two bands in the CD spectrum: a positive maximum centered at 16 400 cm^{-1} (610 nm) and a negative maximum centered at 13 000 cm^{-1} (770 nm). The asymmetry of the positive band centered at 16 400 cm^{-1} and the inflection at 18 800 cm^{-1} (532 nm) suggest that an additional positive CD band may be present near 18 800 cm^{-1}. This CD spectrum is in good agreement with those appearing elsewhere.[16-22]

We assign the bands in the near-UV difference spectrum, ($Cu^{II}_2Zn^{II}_2BE$ minus apoprotein) in Figure 1A to ligand-to-metal charge transfer (LMCT) transitions at the native Cu binding site of erythrocuprein (see Table I). Transitions involving Zn^{II} can be ruled out because Zn^{II} complexes have absorption bands at energies less than 50 000 cm^{-1} (λ >200 nm) only when they contain very oxidizable ligands such as I$^-$. In addition, the difference absorption spectrum in Figure 1A resembles the absorption spectra of well-characterized model compounds having tetragonal Cu^{II}–imidazole (ImH) and Cu^{II}–imidazolate (Im$^-$) chromophores.[25]

The UV spectra of tetragonal Cu^{II}–ImH chromophores have been shown by Fawcett et al.[25] to be comprised of three transitions that originate from the σ-symmetry nitrogen-donor lone pair and from two π-symmetry ring orbitals, one having primarily carbon character (π_1) and the other having nitrogen character (π_2). These σ(ImH) → Cu^{II}, π_2(ImH) → Cu^{II}, and π_1(ImH) → Cu^{II} LMCT absorptions were reported at 45 500 (220), 38 500 (260), and 30 300 cm^{-1} (330 nm), respectively.[25] The position of the latter two bands is similar to those observed in the near-UV difference spectrum of $Cu^{II}_2Zn^{II}_2BE$ (Figure 1) and suggests that they may have similar origins. The broadness of these bands is believed to be due to ligand rotation about the Cu–N σ bond.[25] The close correspondance between the band positions in the near-UV CD spectrum of $Cu^{II}_2Zn^{II}_2BE$ and the absorption spectrum of the protein with the apoprotein contribution subtracted out indicates that the Cu^{II} charge-transfer bands dominate the near-UV CD spectrum as previously postulated.[16]

A closer look at the weaker absorption and CD bands of $Cu^{II}_2Zn^{II}_2BE$ in the near-UV and visible region is shown in Figure 2. The extra band at 24 000 cm^{-1} (417 nm) in the optical spectra of $Cu^{II}_2Zn^{II}_2BE$ is not present in spectra of Cu^{II}–ImH chromophores. But a similar broad absorption at 26 700 cm^{-1} (375 nm) was shown by Fawcett et al.[25] to be characteristic of tetragonal Cu^{II}–imidazolate complexes. A red shift in the position of this band to 417 nm in $Cu^{II}_2Zn^{II}_2BE$ is reasonable in light of the suggested distortion away from tetragonal toward tetrahedral[31] or pentacoordinate geometries[23,32-34] for the native Cu site. In addition, it has been suggested[24] that Cu^{II} may not lie in the plane of the imidazolate ring in $Cu^{II}_2Zn^{II}_2BE$ as a result of steric constraints that are not present in model complexes. Such a distortion could also lower the energy of this transition. We therefore assign the 417-nm band in $Cu^{II}_2Zn^{II}_2BE$ to an imida-

(30) Gillard, R. B. In "Physical Methods in Advanced Inorganic Chemistry"; Hill, H. A. O., Day, P., Eds.; Wiley-Interscience: London, 1968; pp 167–213.

(31) Blumberg, W. E.; Peisach, J.; Eisenberger, P.; Fee, J. A. *Biochemistry* **1978**, *17*, 1842–1846.

(32) Morpurgo, L.; Giovagnoli, C.; Rotilio, G. *Biochim. Biophys. Acta* **1973**, *322*, 204–210.

(33) Rotilio, G.; Morpurgo, L.; Calabrese, L.; Finazzi-Agrò, A.; Mondovì, B. In "Metal–Ligand Interactions in Organic Chemistry and Biochemistry", Part 1; Pullman, B., Goldblum, N., Eds.; Reidel: Dordrecht, Holland, 1977; pp 243–253.

(34) Richardson, J. S.; Thomas, K. A.; Rubin, B. H.; Richardson, D. C. *Proc. Natl. Acad. Sci. U.S.A.* **1975**, *72*, 1349–1353.

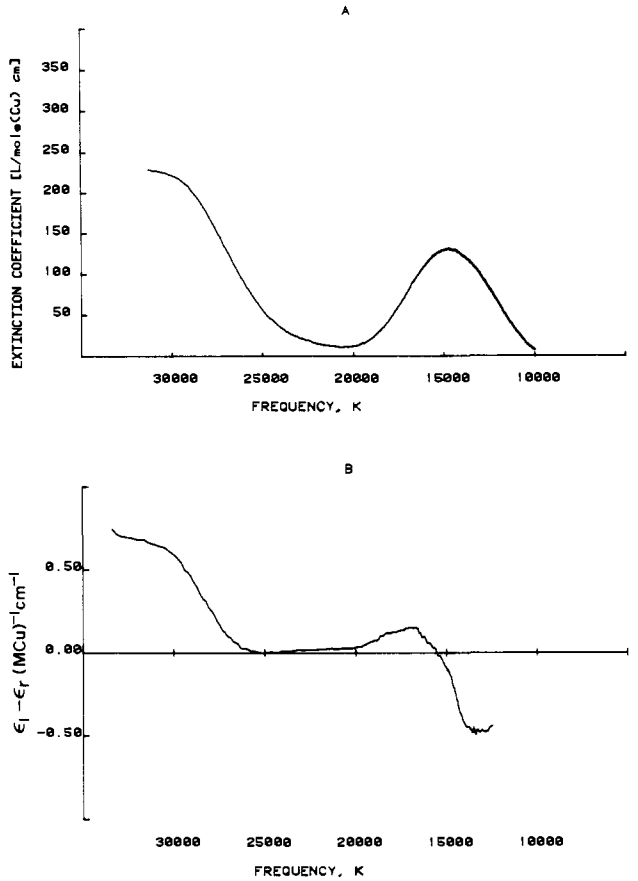

Figure 3. (A) Visible and near-IR absorption spectrum of $Cu^{II}_2E_2BE$ at pH 3.6. This spectrum was obtained with a 0.85 mM (subunits) solution of the Zn-free protein in 50 mM potassium phosphate. (B) Visible and near-IR circular dichroism spectrum of $Cu^{II}_2E_2BE$ at pH 3.6. The same protein solution described above was used to obtain this CD spectrum. See Experimental Section for details.

zolate → Cu^{II} LMCT transition. It had previously been assigned to a d–d transition,[19] presumably due to its low intensity. Our assignment is supported by the observation that this band is not present in the absorption and CD spectra of $Cu^{II}_2E_2BE$ (see below).

The assignment of the broad band at 24 000 cm^{-1} (417 nm) in the absorption and CD spectra of $Cu^{II}_2Zn^{II}BE$ to an Im– → Cu^{II} LMCT band provides further evidence that an imidazolate ligand bridges Cu^{II} and Zn^{II} *in solution.* Direct evidence for an imidazolate bridge in $Cu^{II}_2Zn^{II}_2BE$ has recently been obtained by using electron spin–echo spectroscopy.[35a] Other evidence for the existence of an imidazolate bridge in solutions of derivatives of erythrocuprein comes from a comparison of the temperature dependence of the ESR spectrum of $Cu^{II}_2Cu^{II}_2BE$[35b] with the magnetic and ESR properties of a binuclear imidazolate-bridged Cu^{II} model complex[36] that was characterized by X-ray diffraction techniques. In each case an antiferromagnetic exchange interaction was found with a coupling constant of $J \simeq -25$ cm^{-1}. But evidence for the existence of an imidazolate bridge in $Cu^{II}_2Cu^{II}_2BE$ does not necessarily mean that it exists in $Cu^{II}_2Zn^{II}_2BE$ since Cu^{II} has geometric preferences that differ from those of Zn^{II}. It should be noted that the 417-nm band also appears in the visible absorption spectrum of $Cu^{II}_2Cu^{II}_2BE$[12,13] and of all other binuclear derivatives in which a divalent metal ion is substituted for Zn^{II}, i.e., $Cu^{II}_2Co^{II}_2BE$, $Cu^{II}_2Cd^{II}_2BE$, and $Cu^{II}_2Hg^{II}_2BE$[23], suggesting that imidazolate also bridges the two metals in each subunit of these derivatives. (Our conclusion that Cu^{II} and Cd^{II} are bridged by imidazolate in $Cu^{II}_2Cd^{II}_2BE$ differs from the conclusion of Bauer et al.[37] for the Cd^{II}-substituted yeast protein.)

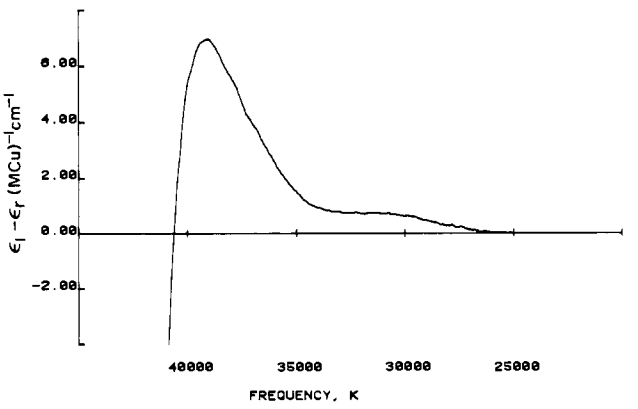

Figure 4. Near-UV circular dichroism spectrum of $Cu^{II}_2E_2BE$ at pH 3.6. The protein solution was the same as that described in Figure 3.

The positive Cotton effect at 16 400 cm^{-1} (610 nm) and the negative Cotton effect at 13 000 cm^{-1} (770 nm) have been previously assigned to Cu^{II} d–d transitions.[19] The asymmetry of the positive band centered at 16 400 cm^{-1} and the inflection near 18 800 cm^{-1} (532 nm) suggest that another positive Cotton effect exists near 18 800 cm^{-1}. The inflection appears in almost every published CD spectrum of $Cu^{II}_2Zn^{II}_2BE$ but has apparently been ignored. The position of this band implies that it is a third d–d transition. No corresponding inflection is detected in the absorption envelope.

Optical Properties of $Cu^{II}_2E_2BE$. The visible–UV absorption and CD spectra of zinc-free erythrocuprein ($Cu^{II}_2E_2BE$) at pH 3.6 are presented in Figure 3. The most obvious differences from the spectra of $Cu^{II}_2Zn^{II}_2BE$ (Figure 2, A and B) are (1) the absence of the broad shoulder at 24 000 cm^{-1}, (2) an approximately 2500-cm^{-1} blue shift in the position of the lowest energy UV band to 32 000 cm^{-1} (313 nm), and (3) a decrease in the rotational strength of the CD bands in the ligand-field region. A small blue shift in the position of these positive and negative Cotton effects to 17 000 (588) and 13 500 cm^{-1} (741 nm), respectively, is also apparent, in agreement with a slight blue shift in the absorption maximum to 14 800 cm^{-1} (675 nm).

The near-UV CD spectrum of $Cu^{II}_2E_2BE$ at pH 3.6 is shown in Figure 4. Comparison with that of $Cu^{II}_2Zn^{II}_2BE$ (Figure 1B) shows that in addition to the blue shift in the position of the 29 500-cm^{-1} band of $Cu^{II}_2Zn^{II}_2BE$, there is an apparent increase in the rotational strength for the large 39 000-cm^{-1} band and a disappearance or blue shift of the shoulder at 35 000 cm^{-1}.

The effect on the Cu site of removing Zn^{II} from $Cu^{II}_2Zn^{II}_2BE$ at low pH[12] can be seen by comparing Figures 3 and 4 with Figures 1 and 2. The CD spectrum of $Cu^{II}_2E_2BE$ at pH 3.6 in the ligand-field region (see Figure 3B) is greatly diminished from that of $Cu^{II}_2Zn^{II}_2BE$ (see Figure 2B), suggesting that a substantial difference exists in the microenvironment of the Cu^{II} chromophore in these two protein derivatives. The substitution of a water ligand for an imidazole seems unlikely since the CD for $Cu^{II}_2E_2BE$ compared with that of $Cu^{II}_2Zn^{II}_2BE$ in the region of ImH → Cu^{II} LMCT bands (Figure 4) is increased rather than decreased. In addition, there is a small blue shift in the position of the Cotton effects in the ligand-field region of $Cu^{II}_2E_2BE$ at pH 3.6 compared with those of $Cu^{II}_2Zn^{II}_2BE$, which is the opposite of what is expected for the simple substitution of oxygen for a nitrogen ligand-donor atom. A small blue shift in the absorption maximum in the ligand field region for $Cu^{II}_2E_2BE$ to 14 800 cm^{-1} (675 nm) is less apparent.

We conclude that four imidazoles remain coordinated to Cu^{II} in $Cu^{II}_2E_2BE$ at pH 3.6. The ESR parameters for this species were found[13,38] to be quite normal for tetragonal $Cu^{II}N_4$ centers;[39]

(35) (a) Fee, J. A.; Peisach, J.; Mims, W. B. *J. Biol. Chem.* **1981**, *256*, 1910–1914. (b) Fee, J. A.; Briggs, R. G. *Biochim. Biophys. Acta* **1975**, *400*, 439–450.

(36) O'Young, C. L.; Dewan, J. C.; Lilienthal, H. R.; Lippard, S. J. *J. Am. Chem. Soc.* **1978**, *100*, 7291–7300.

(37) Bauer, R.; Demeter, I.; Hasemann, V.; Johansen, J. T. *Biochem. Biophys. Res. Commun.* **1980**, *94*, 1296–1302.

(38) Pantoliano, M. W. Ph.D. Dissertation, Rutgers University, 1980.

(39) Peisach, J.; Blumberg, W. E. *Arch. Biochem. Biophys.* **1974**, *165*, 691–708.

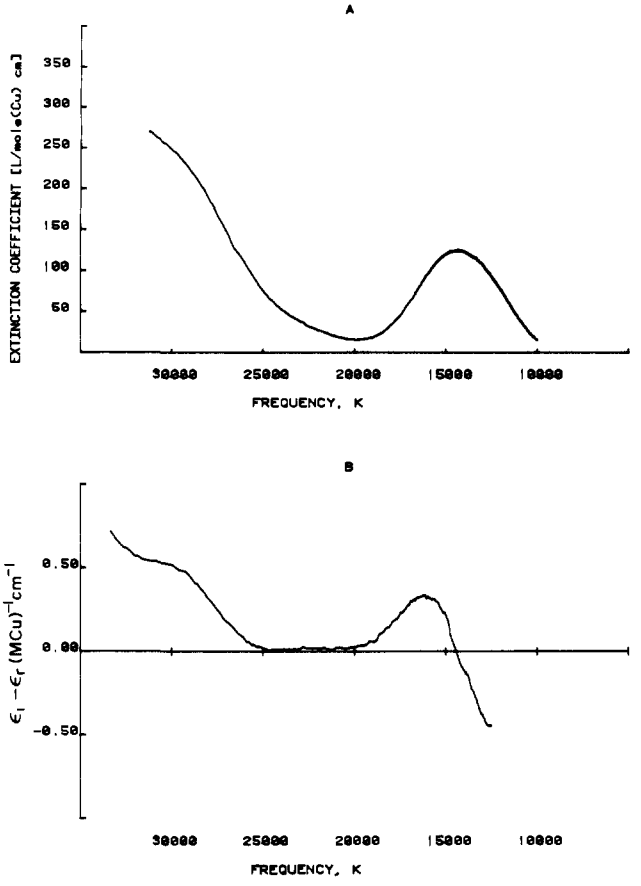

Figure 5. (A) Visible and near-IR absorption spectrum of $Cu^{II}_2E_2BE$ at pH 6.7. This spectrum was obtained with the same protein solution described in Figure 3 except that the pH was adjusted up with 1 M NaOH (extinction coefficient is corrected for dilution). (B) Visible and near-IR circular dichroism spectrum of $Cu^{II}_2E_2BE$ at pH 6.7. The protein solution was the same as described above for (A).

$g_\parallel = 2.260$, $A_\parallel = 15.8 \times 10^{-3}$ cm^{-1} (149 G), and $g_m = 2.067$ with no rhombic contribution detectable at 9 GHz. Thus, the blue shift and decrease in rotational strength of the ligand field bands, together with a decrease in the rhombic character of the ESR spectrum of $Cu^{II}_2E_2BE$ at pH 3.6 compared with those of $Cu^{II}_2M^{II}_2BE$ derivatives, strongly suggest that the Cu^{II} of $Cu^{II}_2E_2BE$ exists in a more nearly regular tetragonal ligand field in the absence of divalent metal ions bound at the native Zn^{II} site. An idealized square-planar geometry around Cu^{II} in $Cu^{II}_2E_2BE$ at pH 3.6 is unlikely, however, because the square-planar complex $Cu(ImH)_4^{2+}$ has a ligand-field maximum near 16 100[26] to 16 700 cm^{-1} [31] (600 nm) with ϵ 50 M^{-1} cm^{-1} and an axial ESR signal characterized by $A_\parallel = 18.0 \times 10^{-3}$ cm^{-1}.[40] A small tetrahedral distortion of these four ligands,[5] or, alternatively, a pentacoordinate square-pyramidal structure[41,42] with water as a fifth apical ligand are more consistent with the optical[43,44] and ESR[45] data.

As described elsewhere,[13] the ligand-field absorption envelope of $Cu^{II}_2E_2BE$ has been observed to undergo a pH-dependent shift in position and intensity in the range $3.5 \leq$ pH ≤ 7.0 with an apparent midpoint at pH 5.0. The CD spectrum of $Cu^{II}_2E_2BE$ at pH 6.7 also differs from that at pH 3.6. The CD and absorption spectra at pH 6.7 are shown in Figure 5. Increasing the pH of solutions of $Cu^{II}_2E_2BE$ from 3.6 to 6.7 causes the following changes to occur in the CD spectrum: (1) There is a red shift in the position of the broad UV band at 32 000 (313) to 31 000 cm^{-1} (323 nm). [The position of this band in Cu_2E_2BE at pH 6.7 is therefore closer to where it is found in $Cu^{II}_2Zn^{II}_2BE$ (29 500 cm^{-1}).] (2) There is an overall increase in the rotational strength of the Cotton effect(s) between 14 000 and 20 000 cm^{-1} and an apparent red shift to 16 200 cm^{-1} (617 nm). [The position and rotational strength of this band for $Cu^{II}_2E_2BE$ at pH 6.7 thus more closely resemble those of $Cu^{II}_2Zn^{II}_2BE$ (see Figure 2B). The asymmetry of this band also resembles that of $Cu^{II}_2Zn^{II}_2BE$ and suggests that a smaller positive Cotton effect may be present on the high-energy side near 18 500 cm^{-1} (551 nm).] (3) There is also a red shift in the position of the negative Cotton effect, and its maximum appears to be at an energy less than 12 500 cm^{-1} ($\lambda > 800$ nm). The red shift in the low-energy absorption maximum of $Cu^{II}_2E_2BE$ from 14 700 cm^{-1} (680 nm) at pH 3.6 to 14 300 cm^{-1} (700 nm) at pH 6.7 has been previously reported.[12,13]

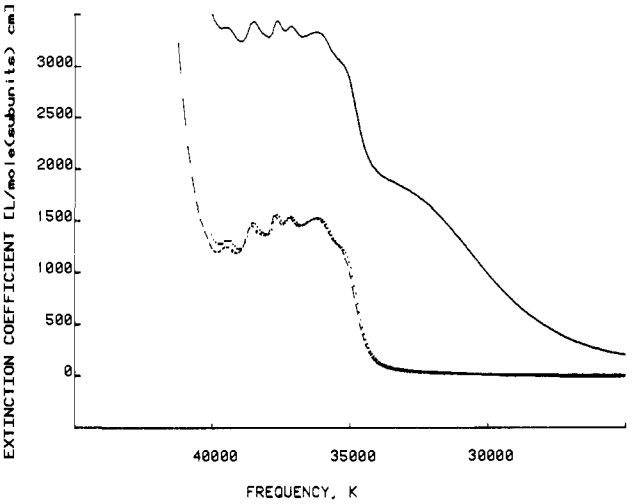

Figure 6. Near-UV absorption spectra of apoprotein before and after titration with Ag^+ and Cu^+: (---) apoprotein (0.27 mM) in 10 mM sodium acetate at pH 3.7; (···) apoprotein after titration with 1.0 equiv of $AgNO_3$/subunit and subsequent dialysis against 1 L of 50 mM potassium phosphate at pH 7.9 (see text); (—) the Ag–apoprotein at pH 7.9 after titration with 1.0 equiv of $CuSO_4$/subunit. The extinction coefficients are based on the concentration of protein subunits and have been corrected for dilution during titration and dialysis.

The visible CD spectrum of $Cu^{II}_2E_2BE$ at pH 6.7 in Figure 5B is significantly different from that at pH 3.6. The increase in the rotational strength of the bands in the ligand-field region of $Cu^{II}_2E_2BE$ reflects an increase in dissymmetry in the microenvironment of the Cu^{II} locus.[46] The red shift in the position of these bands upon increasing the pH parallels the red shift in the ligand-field maximum in the absorption spectrum observed here and elsewhere.[13] The ESR spectrum of $Cu^{II}_2E_2BE$ was also observed to become more rhombic with a concomitant decrease in $A_\parallel$ as the pH was increased from 3.6 to 7.0.[13,38] Together, these pH-dependent changes in the optical and ESR spectral properties suggest that the coordination geometry of the Cu^{II} binding site is altered in the pH range 3.6–7.0. One of the most striking differences between the properties of $Cu^{II}_2E_2BE$ at pH 3.6 and near neutral pH is its greatly reduced affinity for divalent metal ions at low pH[12,13] It is interesting to speculate that the pH-dependent spectral changes observed for $Cu^{II}_2E_2BE$ are related to the physical changes that cause the reduction in metal binding affinity of the Zn site.

Optical Properties of $Ag^I_2Cu^{II}_2BE$. Substitution of Cu^{II} for Zn^{II} at the zinc binding site of erythrocuprein was accomplished essentially as described by Beem et al.[24] It was found that addition of 1 equiv per subunit of an aqueous $AgNO_3$ solution to an apoprotein solution buffered at pH 3.8 with 10 mM sodium acetate produced no UV spectral changes. Dialysis of this silver–apo-

(40) Malmström, B. G.; Vänngård, T. *J. Mol. Biol.* **1960**, *2*, 118–124.
(41) Tomlinson, A. A. G.; Hathaway, B. J. *J. Chem. Soc. A* **1968**, 1905–1909.
(42) Tomlinson, A. A. G.; Hathaway, B. J. *J. Chem. Soc. A* **1968**, 2578–2583.
(43) Hathaway, B. J.; Tomlinson, A. A. G. *Coord. Chem. Rev.* **1970**, *5*, 1–43.
(44) Hathaway, B. J.; Billing, D. E. *Coord. Chem. Rev.* **1970**, *5*, 143–207.
(45) Hathaway, B. J. *J. Chem. Soc., Dalton Trans.* **1972**, 1196–1199.
(46) For a review of CD and MCD of metalloenzymes, see: Vallee, B. L.; Holmquist, B. In "Advances in Inorganic Biochemistry"; Darnall, D. W., Wilkins, R. G., Eds.; Elsevier: New York, 1980; Vol. 2, pp 27–74.

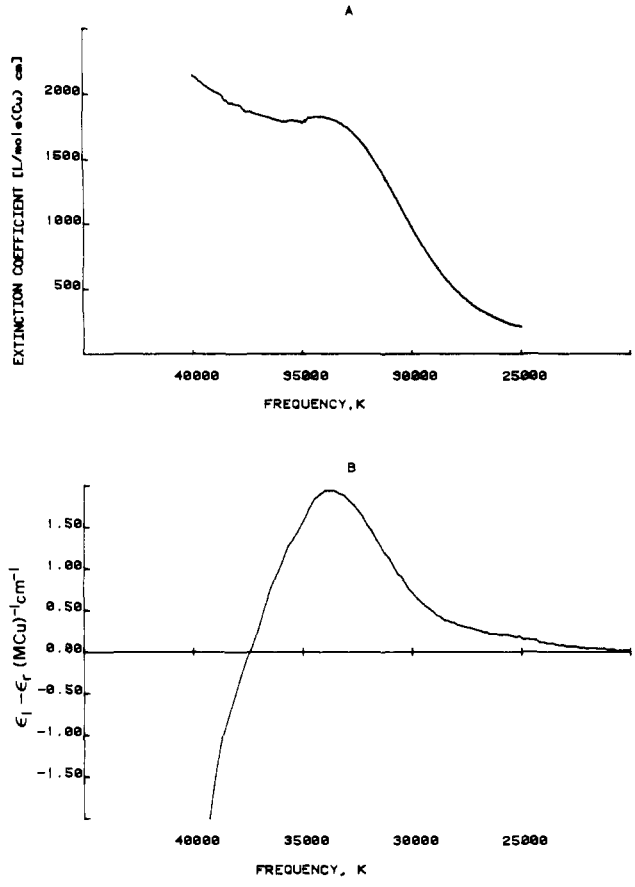

Figure 7. (A) $Ag^{I}_2Cu^{II}_2BE$ minus apoprotein difference spectrum generated by digitally subtracting the two corresponding spectra in Figure 6. (B) Near-UV circular dichroism spectrum of the Ag–Cu protein at pH 7.1. This spectrum was obtained with a 0.9 mM (subunits) solution of $Ag^{I}_2Cu^{II}_2BE$ in 0.1 M potassium phosphate. A lyophilized sample of the protein was used in the preparation of this solution.

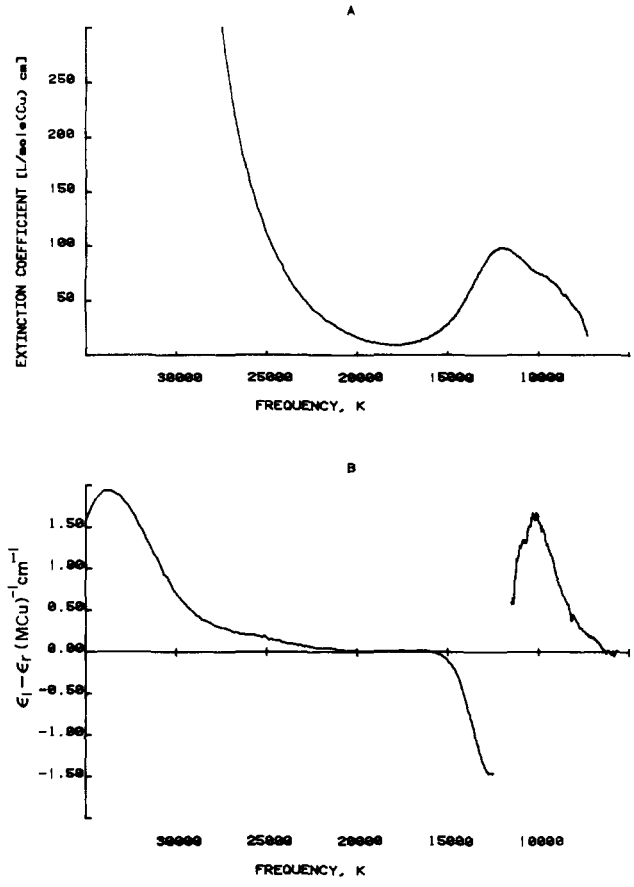

Figure 8. (A) Visible and near-IR absorption spectrum of $Ag^{I}_2Cu^{II}_2BE$ at pH 7.1. The protein solution used in this case was the same one described in Figure 7B. (B) Visible and near-IR circular dichroism spectrum of the Ag–Cu protein. The same protein solution described in (A) was used to obtain the CD spectrum at energies >12 500 cm^{-1} (λ < 800 nm). For the spectral measurements at energies <12 500 cm^{-1}, a 0.4 mM (subunits) solution of $Ag^{I}_2Cu^{II}_2BE$ in D_2O at pH 6.2 was used (see text). The absence of data between 12 500 and 11 500 cm^{-1} (800 and 870 nm) is due to the inability of either of the two spectropolarimeters used to make reliable measurements in this region of the spectrum.

protein solution against 50 mM potassium phosphate solution at pH 7.9 also caused no spectral changes. The resulting spectrum (Figure 6) is almost identical with that of the apoprotein. Addition of 1 equiv per subunit of an aqueous $CuSO_4$ solution to the silver–apoprotein solution resulted in a dramatic increase in the UV absorption (Figure 6). Digital subtraction of the apoprotein spectrum from that of the silver–copper protein spectrum resulted in the difference spectrum shown in Figure 7A. It consists of a very broad and moderately intense band ($\Delta\epsilon$ = 1800 M^{-1} cm^{-1}) at 34 000 cm^{-1} (294 nm). Another broad and more intense band is apparent at higher energy [frequency > 40 000 cm^{-1} (λ < 250 nm)]. The near-UV CD spectrum of the silver–copper protein is shown in Figure 7B. It is comprised of a minimum of two Cotton effects. A weak positive Cotton effect can be discerned near 26 500 cm^{-1} (377 nm) as a shoulder on a much larger positive Cotton effect with a maximum at 33 800 cm^{-1} (296 nm). The position and breadth of this large Cotton effect closely resemble those of the moderately intense band in the absorption difference spectrum. This observation indicates that the near-UV CD spectrum of the silver-copper protein is dominated by the Cu^{II} chromophore as was found for $Cu^{II}_2Zn^{II}_2BE$ as well (vide supra).

The $Ag^{I}_2Cu^{II}_2BE$ minus apoprotein UV difference spectrum (Figure 7A) shows charge-transfer bands that are clearly different from those of $Cu^{II}_2Zn^{II}_2BE$ or $Cu^{II}_2E_2BE$. Comparison of the near-UV spectrum of $Ag^{II}_2Cu^{II}_2BE$ (Figure 6) with that of $Cu^{II}_2Cu^{II}_2BE$[13,38] reveals that both proteins contain a moderately intense (ϵ = 2000 M^{-1} cm^{-1}) and very broad band at 33 300 cm^{-1} (300 nm). This observation suggests that the band is characteristic of Cu^{II} bound at the zinc binding site. The origin of this band is presumably ligand → Cu^{II} charge transfer in nature since it appears only upon the addition of Cu^{2+} to $Ag^{I}_2E_2BE$ or to $Cu^{II}_2E_2BE$. In this case, it is necessary to consider carboxylate (COO^-) and imidazole as potential sources of LMCT transitions. In this regard, a very broad and asymmetric band at 39 100 cm^{-1} (256 nm) and of moderate intensity (ϵ = 3000 M^{-1} cm^{-1}) has been demonstrated for solutions of copper acetate[47] and has been assigned to n(s,p) of carboxylate → Cu^{II} LMCT. The possibility of such a band red shifting to the vicinity of 33 300 cm^{-1} (300 nm) is not unreasonable in light of the significant distortion from tetragonal toward tetrahedral or pentacoordinate geometry that is evident from the ligand-field and ESR spectra for the Cu^{II} ion in $Ag^{I}_2Cu^{II}_2BE$ (see below). Of course, the ImH → Cu^{II} charge-transfer bands may be similarly red shifted from their position in tetragonal complexes so that the broad absorption at 300 nm in the spectra of $Ag^{I}_2Cu^{II}_2BE$ and $Cu^{II}_2Cu^{II}_2BE$ is most likely due to a superposition of π(ImH) → Cu^{II} and n(s,p) (COO^-) → Cu^{II} LMCT transitions.

The silver–copper protein solution was exhaustively dialyzed against doubly distilled deionized water and lyophilized to give a dry colorless powder that was stored under argon in the dark at −20 °C. Analysis of this powder by atomic absorption photometry revealed that it contained 1.04 ± 0.03 equiv of Cu^{II} per subunit. Some of the lyophilized sample of the silver–copper protein was dissolved in 50 mM potassium phosphate buffer (pH 7.1) to give a solution that was 0.90 mM in subunits. This solution was filtered to remove a small amount of undissolved protein and then used to obtain the absorption and CD spectra shown in Figure 8, A and B, respectively. The near-IR CD data at energies less

(47) Dubicki, L.; Martin, R. L. *Inorg. Chem.* **1966**, *5*, 2203–2209.

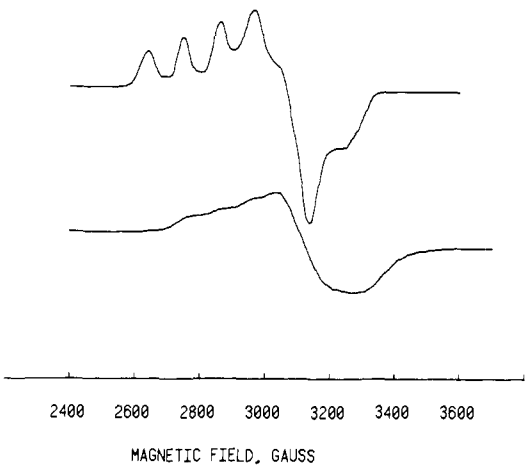

Figure 9. The ESR spectrum of $Ag^{I}_2Cu^{II}_2BE$ at liquid nitrogen (top) and ambient temperature (bottom). These spectra were obtained for the same solution, which was 1.25 mM (subunits) in D_2O (99.8%) at pH 5.3. The instrument settings for the low-temperature spectrum were as follows: microwave power = 10 mW, microwave frequency = 9.15 GHz, modulation amplitude = 1.0 G, receiver gain = 2500, field modulation = 100 kHz, time constant = 0.3 s, and sweep rate = 180 G/min. The ESR parameters for this spectrum are: $g_z = 2.316$, $g_y = 2.118$, $g_x \simeq 2.01$, and $A_z = 11.6 \times 10^{-3}$ cm^{-1}. The instrument settings for the ambient-temperature spectrum (~30 °C) were as follows: microwave power = 10 mW, microwave frequency = 9.41 GHz, modulation amplitude = 100 G, receiver gain = 5000, field modulation = 100 kHz, time constant = 1.0 s, sweep rate = 90 G/min. The ESR parameters for this spectrum are $g_z = 2.289$, $g_y = 2.152$, $g_x \simeq 2.01$, and $A_z = 10.2 (\pm 0.5) \times 10^{-3}$ cm^{-1}.

than 11 500 cm^{-1} ($\lambda > 870$ nm) were obtained by using a sample of lyophilized silver–copper protein that was dissolved in D_2O (99.8% D) and dialyzed exhaustively against this solvent at room temperature. The resulting pH of this solution was found to be 6.2 (uncorrected). [D_2O was used as the solvent because overtone bands from H_2O vibrational modes strongly absorb at frequencies less than 7700 cm^{-1} ($\lambda > 1300$ nm).]

The ligand-field regions of both the absorption and CD spectra of $Ag^{I}_2Cu^{II}_2BE$ are shown in Figure 8. The CD data are in agreement with the absorption data since three Cotton effects in the near IR are clearly discernible: a negative one near 12 300 cm^{-1}, a positive one near 10 000 cm^{-1}, and a positive inflection near 7700 cm^{-1}. (The positive inflection near 11 000 cm^{-1} is not believed to be real due to the great amount of noise in that region of the spectrum.) A preliminary Gaussian-resolution analysis showed that this region of the CD spectrum can be resolved into a minimum of three bands at 12 200, 10 200, and 8000 cm^{-1} with bandwidths at half-height of ~2500 cm^{-1}. The widths of these bands are consistent with d–d bands, but their positions are considerably red shifted from those of tetragonal Cu^{II} complexes. If one assumes that the same four ligands that bind Zn^{II} are also bound to Cu^{II} (N_3O ligand donor set), the red shift of the d–d bands is consistent with a significant deviation from square planar toward tetrahedral coordination geometry as was suggested for Cu^{II}-substituted carboxypeptidase A (Cu^{II}CPA).[5] The deviation from planarity appears to be greater for $Ag^{I}_2Cu^{II}_2BE$ than for Cu^{II}CPA or most other reported Cu^{II}-substituted zinc metalloproteins[48] since the d–d bands of $Ag^{I}_2Cu^{II}_2BE$ are further red-shifted in spite of an apparently stronger ligand field (N_3O vs. N_2O_2 for CPA). Support for this supposition comes from ESR spectral measurements at liquid-nitrogen and room temperatures (30 °C) (see Figure 9), which reveal hyperfine coupling constants ($A_\parallel$) of 11.6×10^{-3} cm^{-1} and $10.2 \pm 0.5 \times 10^{-3}$ cm^{-1}, respectively. These are unusually low values of $A_\parallel$ for tetragonal Cu^{II} complexes but can be understood in terms of a flattened tetrahedral geometry.[49,50]

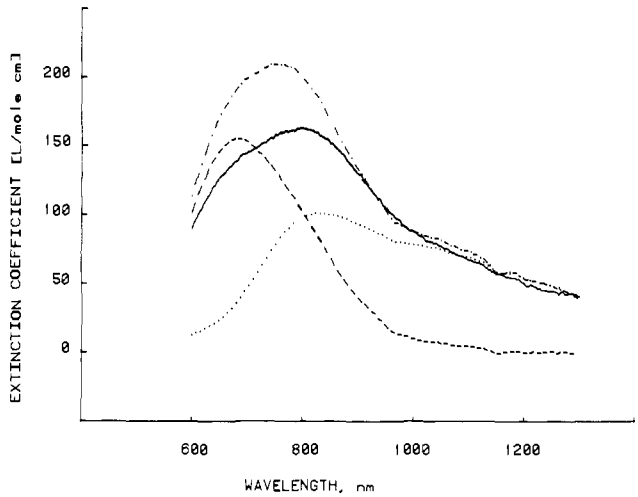

Figure 10. Comparison of the near-IR absorption spectrum of $Cu^{II}_2Cu^{II}_2BE$ (—) with that of $Cu^{II}_2Zn^{II}_2BE$ (---) and the Ag–Cu protein (···). The extinction coefficients for the latter two protein derivatives were based on the amount of Cu determined by AA analysis so that the units are M(Cu)$^{-1}$ cm^{-1}. The extinction coefficient for $Cu^{II}_2Cu^{II}_2BE$ derivative as a function of λ is based on the concentration of protein subunits, which was 0.42 mM in unbuffered water (pH 5.4). A digital addition of the $Cu^{II}_2Zn^{II}_2BE$ and Ag–Cu protein spectra generated the spectrum with the dot–dash (–·–) designation.

While the optical and ESR spectral properties suggest a flattened tetrahedral geometry for Cu^{II} bound at the Zn site of erythrocuprein, a distorted pentacoordinate geometry cannot be ruled out on the basis of the present data. Bencini et al.[51] have shown that pentacoordinate Cu^{II} complexes with geometries intermediate between a square-based pyramid and a trigonal bipyramid can give small $A_\parallel$ values (0.007–0.0013 cm^{-1}) and low-energy ligand-field transitions for N_3O_2 ligand donor sets that compare reasonably well with those for $Ag^{I}_2Cu^{II}_2BE$. Also, intermediate pentacoordinate copper complexes are characterized by strong rhombic distortions as found for $Ag^{I}_2Cu^{II}_2BE$.[51]

In either case, the optical and ESR data strongly suggest that the Cu^{II} at the zinc binding site of erythrocuprein is distorted from planarity to a greater extent than that found for most of the other Cu^{II}-substituted zinc metalloproteins. This observation suggests that the Zn binding site in $Cu^{II}_2Zn^{II}_2BE$ near neutral pH is less flexible under these conditions than those of the other copper-substituted Zn proteins and consequently cannot adjust itself to a more tetragonal geometry preferred by Cu^{II}.

Comparison of the Near-IR Absorption Spectra of $Cu^{II}_2Cu^{II}_2BE$, $Cu^{II}_2Zn^{II}_2BE$, and $Ag^{I}_2Cu^{II}_2BE$. The near-IR absorption spectra of $Cu^{II}_2Cu^{II}_2BE$, $Cu^{II}_2Zn^{II}_2BE$, and $Ag^{I}_2Cu^{II}_2BE$ are compared in Figure 10. An attempt was made to simulate the spectrum of $Cu^{II}_2Cu^{II}_2BE$ by digital addition of the spectra of $Cu^{II}_2Zn^{II}_2BE$ and $Ag^{I}_2Cu^{II}_2BE$. The simulated spectrum is almost identical with that of $Cu^{II}_2Cu^{II}_2BE$ at $\lambda > 850$ nm, although some disparity is evident in the range $600 < \lambda < 850$ nm, partially due, no doubt, to the fact that this sample of $Cu^{II}_2Cu^{II}_2BE$ contained only 1.8 equiv of Cu per subunit. This observation strongly supports the claim of Beem et al.[24] that the Cu^{II} of the silver–copper protein is bound at the native zinc binding site.

Comparison of the ESR Spectra of $Ag^{I}_2Cu^{II}_2BE$ with Those of Other Cu Proteins. One interesting observation concerning the ESR spectrum of $Ag^{I}_2Cu^{II}_2BE$ is that it, along with some other derivatives of erythrocuprein, strongly resembles the spectra of derivatives obtained from modification or partial reduction of tree and fungal laccase and cytochrome *c* oxidase.[52] The ESR signals

(48) The ligand field transitions for Cu^{II}-substituted carboxypeptidase A, carbonic anhydrase, thermolysin, and Ag_2Cu_2BE are compared in ref 38.

(49) Gray, H. B. In "Advances in Inorganic Biochemistry"; Darnall, D. W., Wilkins, R. G., Eds.; Elsevier: New York, 1980; Vol. 2, pp 1–25.

(50) Sakaguchi, U.; Addison, A. W. *J. Chem. Soc., Dalton Trans.* **1979**, 600–608.

(51) Bencini, A.; Bertini, I.; Gatteschi, D.; Scozzafava, A. *Inorg. Chem.* **1978**, *17*, 3194–3197.

(52) Reinhammar, B.; Malkin, R.; Jensen, P.; Karlsson, B.; Andréasson, L. E.; Aasa, R.; Vänngård, T.; Malmström, B. G. *J. Biol. Chem.* **1980**, *255*, 5000–5003.

Table II. ESR Parameters for Cu^{II} Signals Originated from Modified Type 3 Centers[a] Compared with Those of $Cu^{II}_2Zn^{II}_2BE$, $Ag^{I}_2Cu^{II}_2BE$, and $Cu^{I}_2Cu^{II}_2BE$

protein	g_x	g_y	g_z	A_z, 10^3 cm^{-1}
fungal laccase (a)[d]	2.025	2.148	2.268	12.5
tree laccase (b)	2.05	2.150	2.305	7.8
cytochrome oxidase (c)	2.052	2.109	2.278	10.2
$Cu^{II}_2Zn^{II}_2BE$ (d)	2.025	2.103	2.257	13.2
$Ag^{I}_2Cu^{II}_2BE$ (30 °C) (e)	~2.01[c]	2.15	2.289	10.2 ± 0.5
$Cu^{I}_2Cu^{II}_2BE$[b] (f)	~2.02	~2.12	2.31	10.8

[a] Taken from ref 52. [b] $Cu^{II}_2Cu^{II}_2BE$ reduced with ferrocyanide. Taken from ref 35. [c] Estimated from X-band spectrum. [d] Letters refer to data points in Figure 11.

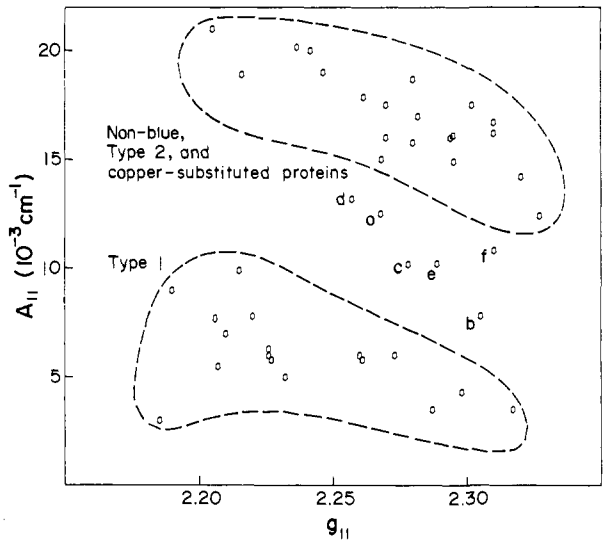

Figure 11. Relationship between $g_{\parallel}$ and $A_{\parallel}$ for naturally occurring copper proteins and copper-substituted metalloproteins. Points designated by letters represent data given in Table II. Other points are from the supplementary material (SUP 22415) for ref 50. Comparison should also be made with Figure 9 of ref 39.

observed in the latter three metalloenzymes are believed to originate from a Cu^{II} ion that is normally ESR nondetectable in the resting enzyme due to strong magnetic interactions ($-J \geq 500$ cm^{-1}) either with another Cu^{II} (laccases) or an Fe^{III} ion (cytochrome *c* oxidase). The ESR parameters for the new copper signals as reported by Reinhammar et al.[52] are compared with those of $Ag^{I}_2Cu^{II}_2BE$, $Cu^{I}_2Cu^{II}_2BE$, and $Cu^{II}_2Zn^{II}_2BE$ in Table II. These ESR signals are strikingly different from those found for nonblue, type 2, or type 1 copper centers of metalloenzymes in that they are characterized by a strong rhombic splitting ($g_y - g_x \geq 0.057$) and a moderately small $A_{\parallel}$ (7.8×10^{-3} to 13.2×10^{-3} cm^{-1}) when compared with tetragonal model complexes. The novelty of these ESR parameters is more fully comprehended when they appear, together with Cu^{II} ESR data for other Cu proteins,[50] on a $g_{\parallel}$ vs. $A_{\parallel}$ plot (see Figure 11). This plot is similar to that originally presented by Peisach and Blumberg[39] and includes the data of Table II. The new type 3 ESR signals and those of $Cu^{II}_2Zn^{II}_2BE$, $Ag^{I}_2Cu^{II}_2BE$, and $Cu^{I}_2Cu^{II}_2BE$ are seen to form a class of their own, which is intermediate between that class of Cu^{II} centers in copper proteins that are characterized by tetragonal ESR and optical properties (nonblue & type 2) and that class of Cu^{II} centers characterized by pseudotetrahedral (or flattened tetrahedral) ESR and optical properties (type 1).[49] The data plotted in Figure 11 suggest that the modified or partially reduced type 3 copper of tree and fungal laccase and cytochrome *c* oxidase centers may be structurally related to the binuclear derivatives of erythrocuprein where Cu^{II} is bound either at the native copper site ($Cu^{II}_2Zn^{II}_2BE$), at the native zinc site ($Ag^{I}_2Cu^{II}_2BE$), or at both metal binding sites ($Cu^{I}_2Cu^{II}_2BE$). It should be emphasized, however, that we do not mean to imply that imidazole bridges the binuclear copper centers in the laccases and cytochrome oxidase—only that a N_4O ligand donor set to Cu^{II} with distorted pentacoordinate geometry[24] ($Cu^{II}_2Zn^{II}_2BE$) and N_3O_2 or N_3O ligand donor set to Cu^{II} with distorted-pentacoordinate or flattened-tetrahedral geometry ($Ag^{I}_2Cu^{II}_2BE$, see above) can simulate the unique ESR spectral properties of modified or partially reduced type 3 copper centers. It should be noted further that $Ag^{I}_2Cu^{II}_2BE$, $Cu^{II}_2Cu^{II}_2BE$, and presumably $Cu^{I}_2Cu^{II}_2BE$ contain moderately intense ($\epsilon \simeq 2000$ M^{-1} cm^{-1}) near-UV bands (~300 nm) not unlike the 330-nm band characteristic of type 3 copper centers in blue oxidases.[53]

Acknowledgment. Financial support from the NSF (J.S.V. and L.A.N.) and the USPHS (GM-28222, J.S.V., and GM-23567, L.A.N.) is gratefully acknowledged. We are especially grateful to Professor H. J. Schugar for helpful discussions and disclosure of results prior to publication.

Registry No. Superoxide dismutase, 9054-89-1; Cu, 7440-50-8.

(53) Solomon, E. I. In "Copper Proteins"; Spiro, T. G., Ed.; Wiley: New York, 1981; pp 41–108.